

Isolated Influence of Microwave Energy and Acidic solution on Wettability Alteration and Hydrocarbon Desorption in Carbonate Reservoir Rocks

Abstract

This study investigates the independent effects of microwave irradiation and acidic solutions on wettability alteration and hydrocarbon desorption in carbonate reservoir rocks. Contact angle measurements and ATR-FTIR spectroscopy were employed to analyze both surface wettability changes and molecular-scale modifications. Microwave treatment at 780 W and 1300 W reduced the contact angle from an initially oil-wet state of $\sim 132^\circ$ to 72° and 69° , respectively, indicating a pronounced shift toward water-wet conditions. FTIR analysis confirmed these observations, showing decreases in the Polar/Aliphatic and Aromatic/Aliphatic indices, which reflect the desorption of polar and aromatic compounds from the rock surface. Acidic solutions produced similar effects, although their efficiency depended on brine composition, hydrochloric acid in deionized water reduced the contact angle to $\sim 57^\circ$, while seawater and formation water resulted in weaker changes due to ionic buffering by Ca^{2+} and Mg^{2+} . The novelty of this work lies in the separation of microwave and acid effects, demonstrating distinct mechanisms. Microwave irradiation enhances desorption through dielectric heating and bond disruption, whereas acidic solutions act primarily through chemical reactivity and ionic competition. These findings show that both methods independently promote wettability alteration, with efficiency governed by microwave power and brine chemistry. The results provide practical insights for the design of advanced Enhanced Oil Recovery (EOR) strategies, including microwave-assisted stimulation and optimized acidizing treatments in carbonate reservoirs.

Keywords: microwave irradiation, acidic solutions, wettability alteration, ATR-FTIR analysis, enhanced oil recovery

1. Introduction

Acidizing is a stimulation technique used in oil and gas wells to enhance hydrocarbon flow by dissolving formation damage and creating new channels, commonly referred to as wormholes. This

26 process aims to rejuvenate production by unclogging blocked pores, improving formation
27 permeability, and ultimately boosting output efficiency [1–3]. Among the key factors influencing
28 fluid behavior in porous media, wettability plays a central role. It directly affects critical reservoir
29 properties such as capillary pressure and relative permeability, thereby exerting a strong influence on
30 fluid distribution and recovery performance [4].

31 Wettability alteration has long been recognized as a critical mechanism in enhancing oil recovery,
32 particularly in carbonate reservoirs, which are often naturally oil-wet due to the strong affinity
33 between rock surfaces and heavy polar components in crude oil. In such systems, shifting the
34 wettability toward a more water-wet condition can significantly improve the efficiency of
35 displacement processes and increase the ultimate recovery factor. Traditional acidizing techniques
36 using hydrochloric acid (HCl) are widely employed to enhance permeability by dissolving carbonate
37 minerals and removing formation damage. However, the effect of acidizing on wettability is often
38 limited or inconsistent, particularly when formation brine contains divalent cations such as Ca^{2+} and
39 Mg^{2+} that can buffer acid reactions and contribute to surface re-oiling or precipitation. To overcome
40 these limitations, researchers have explored various additives such as surfactants, chelating agents,
41 and nanoparticles to enhance acid-rock interactions and promote wettability alteration. Despite some
42 success, challenges such as formation damage, acid sludge formation, and scale precipitation remain
43 concerns in field applications[5].

44 In carbonate reservoirs, acidizing primarily serves to create new flow channels by dissolving both the
45 formation rock and any existing damage, thereby enhancing hydrocarbon production. In contrast,
46 acidizing in sandstone formations is typically aimed at restoring flow by removing damage and
47 blockages without significantly dissolving the rock matrix itself. The key distinction lies in the
48 mechanism: while carbonate acidizing involves the reaction of acid with the reservoir rock itself,
49 sandstone acidizing focuses on dissolving obstructions such as fines and scale that impair
50 permeability. However, acidizing operations in both formations are often challenged by complications
51 such as salt precipitation and the formation of asphaltene sludge. Therefore, careful design and

engineering of the acidizing process is essential to mitigate these risks and improve treatment effectiveness [6].

Matrix acidizing is a stimulation technique used to remove formation damage or enhance permeability in zones located within a few meters of the wellbore. This technique can be applied to both sandstones and carbonates; however, the primary objectives of the operation differ between these two rock types. In carbonates, the aim is to bypass the damaged zone by creating high conductivity channels (wormholes), thereby enhancing the flow of hydrocarbons from the reservoir to the wellbore. In sandstone formations, matrix acidizing operations should primarily aim to remove or dissolve acid-soluble damage or to clear blockages in the perforations and the pore network near the wellbore. Theoretically, the acid flows through the pore system and dissolves solids and fine particles present in the cavities and pore spaces that hinder the flow of oil or gas[7].

In a 2018 study, Yoo et al. examined the dissolution behavior of dolomite in carbonate acidification, focusing on the use of both fresh and spent acids. Spent acid, which results from partial reaction and contains calcium and magnesium ions from the acid-rock interactions, was analyzed separately. The results showed that dolomite dissolved in both types of acid. When comparing the fresh acid with the spent one, it was observed that the spent acid had a higher kinematic viscosity and a lower pH. These differences were linked to a greater dissolution rate and diffusion coefficient in the spent acid, driven by its higher viscosity and lower pH. Furthermore, the study pointed out an unusual ion influence from impurities such as iron oxide and aluminum oxide present in clay, which enhanced the reaction rate, though this was not related to the specific reaction between hydrochloric acid and dolomite [8].

In reservoirs characterized by low permeability and limited heat transfer, electromagnetic (EM) techniques have shown superior performance in reducing oil viscosity and improving fluid mobility compared to conventional methods. Microwaves, a subset of EM waves with frequencies between 300 MHz and 300 GHz, generate an electromagnetic field that selectively transfers energy to materials with high dielectric constants. In petroleum applications, microwaves are most commonly utilized in oil shale and unconventional reservoirs. The heating process is typically implemented by placing a

98 microwave antenna near the production zone. For Enhanced Oil Recovery (EOR), this antenna is
99 installed in a wellbore drilled adjacent to the main production well [9,10]. The presence of
100 microwave-absorbing materials is crucial in these systems, as they significantly influence the
101 efficiency of electromagnetic wave attenuation and energy transfer [11].

102 In their study, Hong et al. utilized formation microwave heat treatment (FMHT) to enhance oil
103 recovery by fracturing the formation. The results revealed a significant increase in the number of
104 fractures as the exposure to microwave energy was extended. These fractures, along with the changes
105 in pore structure induced by microwave treatment, resulted in a reduction in the wave speed (S Pand)
106 within the coal core. The exposure to microwave energy also caused a narrowing of the frequency
107 spectrum range of the coal core. Additionally, the frequency distribution within the spectrum was
108 altered by the microwave radiation. Moreover, a decrease in the coal's density, bulk modulus, and
109 shear modulus was observed following microwave treatment, with the bulk and shear moduli
110 decreasing at a faster rate than the coal's density [12].

111 Electromagnetic (EM) waves are widely used in the petroleum industry for thermal stimulation of oil
112 wells, particularly for enhancing recovery in heavy oil reservoirs. Among their various applications,
113 one of the most significant is the heating of the wellbore region to promote processes such as
114 asphaltene breakdown and crude oil upgrading. Three primary EM-based heating techniques are
115 employed: resistance heating, induction heating, and microwave heating [13].

116 Taheri-Shakib et al. (2018) investigated how microwave irradiation affects the wettability of
117 carbonate reservoir rocks. By examining changes in surface charge and measuring contact angles,
118 they found that extended microwave exposure enhanced the water-wet characteristics of the rock
119 samples [13].

120 Karami et al. (2021) reported that the improvement in rock wettability caused by microwave
121 application is not solely due to thermal effects. Their study revealed that microwave exposure also
122 facilitates the decomposition of organic materials on the rock surface, which weakens van der Waals
123 interactions and leads to noticeable changes in wettability [14].

124 In their 2018 study, Hui Shang et al. examined the effects of microwave irradiation on crude oil

100 viscosity and concluded that the degree of viscosity change depends on the composition and types of
106 compounds present in the oil [15].

107 Of these, microwave heating offers distinct advantages, including minimal energy loss and
108 independence from the surrounding formation's thermal conductivity. In this approach, a microwave-
109 emitting antenna is installed in a wellbore drilled adjacent to the main production well [16-18]. As
110 reservoir fluids migrate toward the production zone, they are directly exposed to microwave radiation,
111 leading to efficient and uniform heating in the vicinity of the well. This localized thermal
112 enhancement helps counteract pressure depletion and significantly lowers the viscosity of heavy and
113 extra-heavy crude oils—ultimately improving reservoir performance and oil recovery rates [19].

114 The use of ATR-FTIR analysis provided crucial insights into the interactions at the rock-fluid
115 interface during acidizing at a molecular level. The results indicated that microwave irradiation
116 significantly boosts the desorption of organic compounds from rock surfaces, such as aromatic
117 hydrocarbons, long-chain alkanes, and polar functional groups including hydroxyl (O-H), amine (N-
118 H), and carbonyl (C=O) groups. This enhanced desorption suggests that microwave energy aids in
119 breaking down complex hydrocarbon structures, which helps in the efficient removal of asphaltene
120 sludge typically formed during acid treatments. Given that asphaltenes are large, high-molecular-
121 weight substances that can block pore spaces and impede fluid flow, microwave-assisted desorption
122 presents a promising technique to improve the performance and effectiveness of acidizing
123 processes[20].

124 In 2023, Le et al. proposed a novel approach for synthesizing zeolite 4A using microwave-assisted
125 techniques, which significantly improved porosity and reduced crystallization time compared to
126 traditional hydrothermal methods. The resulting zeolite 4A displayed high crystallinity, a uniform
127 cubic structure, and an enlarged surface area, as verified by XRD and SEM characterizations.
128 Notably, the process utilized a standard household microwave oven, demonstrating considerable
129 energy savings and suggesting strong potential for industrial application. This method presents a more
130 sustainable and efficient alternative for producing zeolite 4A with enhanced adsorption capabilities
131 [21].

Recent investigations have explored various techniques to enhance oil recovery from carbonate reservoirs, including matrix acidizing, surfactant flooding, and electromagnetic (microwave) stimulation. For instance, several studies reported that microwave heating accelerates oil desorption by disrupting polar and asphaltenic bonds, while others emphasized the role of acid type and brine composition in modifying rock wettability[15,19,20,30].

Despite numerous studies on matrix acidizing and electromagnetic-assisted recovery, the independent (single-variable) influence of microwave power and acid composition on carbonate-rock wettability and hydrocarbon desorption has not been clearly established. Most previous investigations combined chemical and thermal effects, making it difficult to isolate their individual roles. In this study, we systematically decouple these effects by (i) applying 2.45-GHz microwave irradiation at powers of 780 W and 1300 W for 1–11 min, and (ii) performing acid treatments using 15 wt% HCl prepared in deionized water (ADW), synthetic seawater (ASW), and formation water (AFW) for 2–22 min. Wettability was quantified by sessile-drop contact angle, and interfacial chemistry was examined using ATR-FTIR spectral indices (Aromatic/Aliphatic, Polar/Aliphatic, C=O/Aliphatic). The results demonstrate that microwave treatment alone drives a pronounced water-wet shift through the thermal desorption of surface-bound hydrocarbons, whereas acid efficiency is strongly affected by the ionic composition of the base water. These controlled single-factor experiments provide clear mechanistic insight and practical guidance for optimizing wettability alteration in carbonate reservoirs.

2. Materials and method

2.1 Materials

2.1.1 Rock sample

To examine the impact of microwave-assisted acid treatment on the wettability of rock surfaces, a carbonate rock sample was studied. Based on the results from X-ray fluorescence (XRF) analysis shown in Table 1, calcium carbonate (CaCO_3) makes up about 94.50% of the rock's composition. Additional X-ray diffraction (XRD) analysis confirms that the primary mineral in the rock is CaCO_3 . The XRD pattern also indicates the presence of smaller

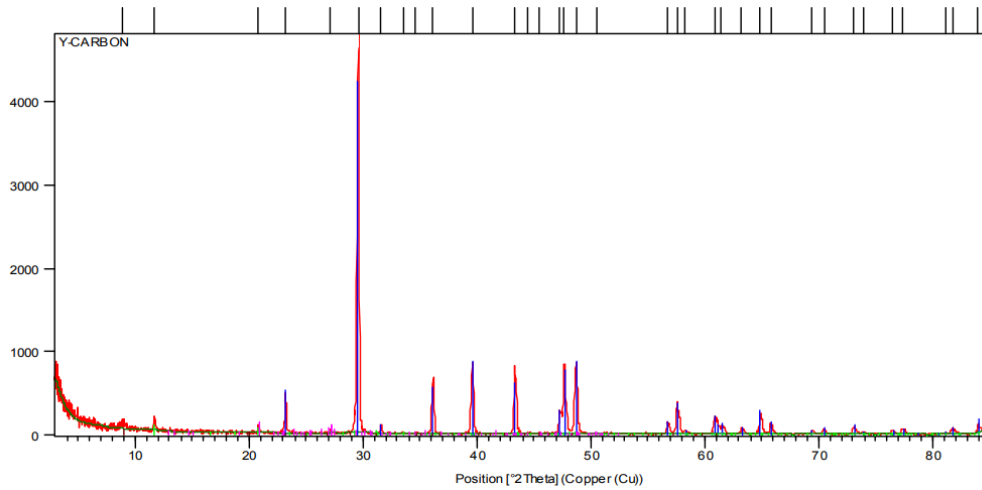
108 quantities of gypsum, microcline, and muscovite. It is important to note that the rock samples
109 analyzed in this research share similar geological characteristics with those studied by
110 Tanhaei et al. (2023). [20]. Figure 1 illustrates the XRD spectrum of the powdered carbonate rock
111 sample.

112

Table 1. The XRF analysis of the rock sample [20]

Mineral	Apparent percentage	LOI	Actual percentage
Na ₂ O	0.035	41.09	0.059413
MgO	0.565	41.09	0.95909
Al ₂ O ₃	0.178	41.09	0.302156
SiO ₂	0.697	41.09	1.183161
P ₂ O ₅	0.081	41.09	0.137498
SO ₃	0.735	41.09	1.247666
Cl	0.009	41.09	0.015278
K ₂ O	0.037	41.09	0.062808
CaO	55.675	41.09	94.50857
TiO ₂	0.067	41.09	0.113733
Fe ₂ O ₃	0.146	41.09	0.247836
Sr	0.684	41.09	1.161093

113



۱۶۴

۱۶۵ Fig 1. The XRD spectrum of the pulverized carbonate rock section. (Also used by Tanhaei et al. 2023
۱۶۶ [20])

۱۶۷ 2.1.2 Oil sample

۱۶۸ The crude oil sample used in this study was obtained from an oil field located in southern Iran. Table
۱۶۹ 2 presents key properties of the oil, including its API gravity, viscosity, acid number, and asphaltene
۱۷۰ content. Furthermore, the detailed compositional analysis of the oil sample utilized in the experiments
۱۷۱ is provided in Table 3[22,23].

۱۷۲ Table 2. API gravity, viscosity, acid number, and asphaltene content of this oil sample[22,23]

Physical properties	API	Viscosity (cP) (@ temperature 26° C)	Acid number	Asphaltene content (%)
Crude oil	20.65 °	37	0.6	16

۱۷۳

۱۷۴ Table 3. The composition of oil sample used for aging the rock sections [20]

Components	Mole weight	Flashed Liquid
Nitrogen	28.01	0
Carbon Dioxide	44.01	0
Hydrogen Sulfide	34.08	0.0004

Methane	16.04	0
Ethane	30.07	0
Propane	44.1	0.139
I – Butane	58.1	0.127
N – Butane	58.12	1.318
I – Pentane	72.15	1.107
N – Pentane	72.15	3.105
Pseudo C ₆ H ₁₄	84	6.109
Pseudo C ₇ H ₁₆	96	9.316
Pseudo C ₈ H ₁₈	107	9.478
Pseudo C ₉ H ₂₀	121	8.252
Pseudo C ₁₀ H ₂₂	134	7.054
Pseudo C ₁₁ H ₂₄	147	6.568
Pseudo C ₁₂ H ₂₆	161	5.547
Pseudo C ₁₃ H ₂₈	175	4.16
Pseudo C ₁₄ H ₃₀	190	3.813
Pseudo C ₁₅ H ₃₂	206	3.12
Pseudo C ₁₆ H ₃₄	222	2.427
Pseudo C ₁₇ H ₃₆	237	2.08
Pseudo C ₁₈ H ₃₈	251	1.733
Pseudo C ₁₉ H ₄₀	263	1.387
Pseudo C ₂₀ H ₄₂	277	1.248
Pseudo C ₂₁ H ₄₄	291	1.04
Pseudo C ₂₂ H ₄₆	305	0.832
Pseudo C ₂₃ H ₄₈	318	0.763
Pseudo C ₂₄ H ₅₀	331	0.693
Pseudo C ₂₅ H ₅₂	345	0.555

Pseudo C26H54	359	0.485
Pseudo C27H56	374	0.416
Pseudo C28H58	388	0.347
Pseudo C29H60	402	0.277
C30+	935	16.666
TOTAL	-	100

۱۷۵

۱۷۶ 2.1.3 Acid solution

۱۷۷ To simulate the early stage of rock-acid interaction during injection, acid solutions with a 15%
 ۱۷۸ concentration were prepared. Three types of base waters—distilled water, seawater, and formation
 ۱۷۹ water—were used in preparing these acid solutions. The composition of the seawater, detailed in
 ۱۸۰ Table 4, is based on the characteristics of water from the Persian Gulf. Furthermore, the formation
 ۱۸۱ water was designed to replicate the chemical properties of the produced water from the reservoir
 ۱۸۲ where the crude oil sample was sourced[20,22,23].

۱۸۳

۱۸۴ Table 4. The composition of brine water compositions (formation water and sea water) [20,22,23]

Composition	Concentration(ppm)		
	Distilled water	Seawater	Formation water
NaCl	0	28323	177465
Na ₂ SO ₄	0	4936	0
CaCl ₂	0	1630	28036
MgCl ₂ . 6H ₂ O	0	10510	6561
KCl	0	1032	3440
TDS	0	46431	215502

۱۸۵

۱۸۶ 2.2 Methods

187 A standard household microwave oven operating at 2.45 GHz with adjustable output power (260–
188 1300 W) was used for irradiation. The temperature of the rock samples was monitored using an
189 infrared thermometer with ± 1 °C accuracy.

190 **2.2.1 Microwave treatment**

191 A typical household microwave oven was used to carry out the microwave treatments. The
192 oven operates at a frequency of 2.45 GHz, with an adjustable power output ranging from 260
193 W to 1300 W. The dimensions of the microwave's internal chamber are 10 × 17 × 20 cm.
194 Like standard microwave devices with a magnetron, this unit emits radiation at a fixed
195 frequency. After immersing the aged rock samples in the prepared acid solutions, they were
196 exposed to microwave radiation at power settings of 780 W and 1300 W for periods between
197 1 and 3 minutes. A control group of similar rock samples was also treated with acid but
198 without microwave exposure, to assess the impact of microwave radiation alone [20,22,23].

199 **2.2.2 Temperature changes**

200 The temperature of the rock sections was measured using a digital laser thermometer (GM-320,
201 Benetech) with an accuracy of ± 1 °C. Since this type of thermometer determines temperature based on
202 infrared radiation reflected from the surface, continuous monitoring during microwave exposure was
203 not feasible. To obtain temperature readings during the microwave treatment, the radiation process
204 was paused at 30-second intervals to allow for measurement. The rock sections were cut to be in a
205 rectangular cube form with the dimensions of 15 cm×10 cm×5 cm[20,22].

206 **2.2.3 Contact Angle Analysis**

207 Wettability plays a crucial role in fluid movement within porous media. To assess the change
208 in wettability of carbonate rock samples before and after treatment, contact angle
209 measurements were conducted. The rock samples, sourced from the previously described
210 carbonate material, underwent thorough cleaning to remove petroleum and salt-based

۲۱۱ contaminants. This cleaning process was carried out using a Soxhlet extractor with methanol
۲۱۲ for two days and toluene for ten days. After cleaning, the rock samples were saturated with
۲۱۳ formation water and subjected to aging at 90°C for two days. Following this, crude oil was
۲۱۴ injected into the water-saturated rock samples, which were then aged in crude oil at 90°C for
۲۱۵ 35 days to simulate reservoir conditions and restore the original wettability [20]. The
۲۱۶ rationale for selecting 90 °C and 35 days for the aging procedure is based on reservoir
۲۱۷ representativeness, mechanistic considerations, and consistency with prior studies. The crude
۲۱۸ oil and carbonate samples used in this work originate from a southern Iranian oilfield with an
۲۱۹ average reservoir temperature of approximately 90 °C. Aging the samples at this temperature
۲۲۰ ensures that oil rock brine interactions occur under conditions closely mimicking the natural
۲۲۱ subsurface environment, allowing for more realistic adsorption of heavy oil fractions
۲۲۲ particularly asphaltenes and resins—onto the carbonate surface. Extended aging for 35 days
۲۲۳ is essential to re-establish the native oil-wet state of carbonate rocks. Previous studies
۲۲۴ (Tanhaei et al., 2023) have shown that shorter durations (<20 days) are insufficient for
۲۲۵ complete adsorption of surface-active components, often leading to mixed-wet conditions
۲۲۶ that do not accurately represent the reservoir. By contrast, 30–40 days of exposure at elevated
۲۲۷ temperature allows heavy polar compounds to strongly adsorb and organize into multilayer
۲۲۸ films, producing a stable oil-wet surface with a baseline contact angle of ~132°.
۲۲۹ Mechanistically, higher temperatures enhance the molecular diffusion and mobility of
۲۳۰ asphaltenes and resins, accelerating their migration toward and binding with calcite sites on
۲۳۱ the rock surface. This thermodynamically favored process is promoted by reduced oil
۲۳۲ viscosity and stronger surface energy interactions. The prolonged duration ensures that
۲۳۳ equilibrium surface coverage is reached, minimizing variability in wettability across replicate
۲۳۴ samples. These aging conditions are also consistent with widely reported protocols in
۲۳۵ carbonate wettability research, where temperatures of 80–100 °C and durations of 30–40 days

are typically adopted. Thus, the selected conditions provide both scientific validity and comparability with prior works. In summary, aging at 90 °C for 35 days replicates in-situ reservoir conditions, enables complete adsorption of polar components, and ensures a stable and reproducible oil-wet baseline for subsequent wettability alteration experiments, so that the observed changes in contact angle and FTIR indices result solely from the applied treatments rather than incomplete wettability restoration[20].

The aged rock sections were then exposed to acid solutions at 70°C for 2-22 min. After acid treatment, microwave radiation was applied for 1- 11 minutes at power levels of 780 and 1300 W. The wettability of the treated rock sections was evaluated using the pendant drop method. Each contact angle measurement was repeated three times, and the median value was reported. The measurements had a precision of $\pm 0.6^\circ$ based on the obtained data.

2.2.4 ATR-FTIR spectrums

Although the sessile-drop contact-angle technique provides valuable information on wettability changes, it does not offer details on the chemical composition of the desorbed hydrocarbons. To address this, Attenuated Total Reflectance-Fourier Transform Infrared (ATR-FTIR) spectroscopy was conducted on the treated rock samples using a refractometer (PerkinElmer, USA). The spectra were recorded within the range of 600–4000 cm^{-1} , with a resolution of 1 cm^{-1} . Quantitative data was extracted from the ATR-FTIR spectra by calculating the integrated areas of the hydrocarbon-related peaks. These values were then used to derive characteristic indexes based on the method proposed by Karami et al. (2022)[20]. Using these indexes, the content of polar, carbonyl, aliphatic, and aromatic functional groups in the rock samples was determined [20].

3. Results and Discussions

3.1 Temperature Changes

209 According to figure 2 ,the temperature evolution of carbonate rock samples under microwave
210 irradiation is illustrated in Fig. 2. After 3 minutes of exposure, the surface temperature of the rock
211 sections rose to approximately 94°C and 120°C under radiation powers of 780 W and 1300 W,
212 respectively. This increase in temperature can be attributed to fundamental electromagnetic heating
213 mechanisms associated with microwave energy. Microwave radiation induces heating primarily
214 through the interaction with polar molecules and materials possessing high dielectric constants. When
215 polar molecules are subjected to an oscillating electromagnetic field, such as that generated by a
216 microwave at 2.45 GHz, the continuous reorientation of their electric dipoles leads to internal friction
217 and, consequently, heat generation. This phenomenon, known as dielectric heating, is especially
218 pronounced in substances with high dielectric loss factors, which quantifies a material's ability to
219 convert electromagnetic energy into thermal energy. Materials with higher dielectric constants and
220 dielectric losses absorb microwave energy more efficiently, resulting in more significant thermal
221 responses. In this study, the observed temperature increase in rock sections can be rationalized by
222 their relatively high dielectric constant. For instance, calcium carbonate (CaCO_3), which comprises
223 the majority of the rock sample (approximately 94.5%), has a dielectric constant of approximately 9.2
224. In contrast, crude oil components typically exhibit much lower dielectric constants, ranging from
225 about 1.0 to 4.5 depending on their molecular structure and polarity . Consequently, the rock matrix is
226 more susceptible to microwave-induced heating than the oil phase.

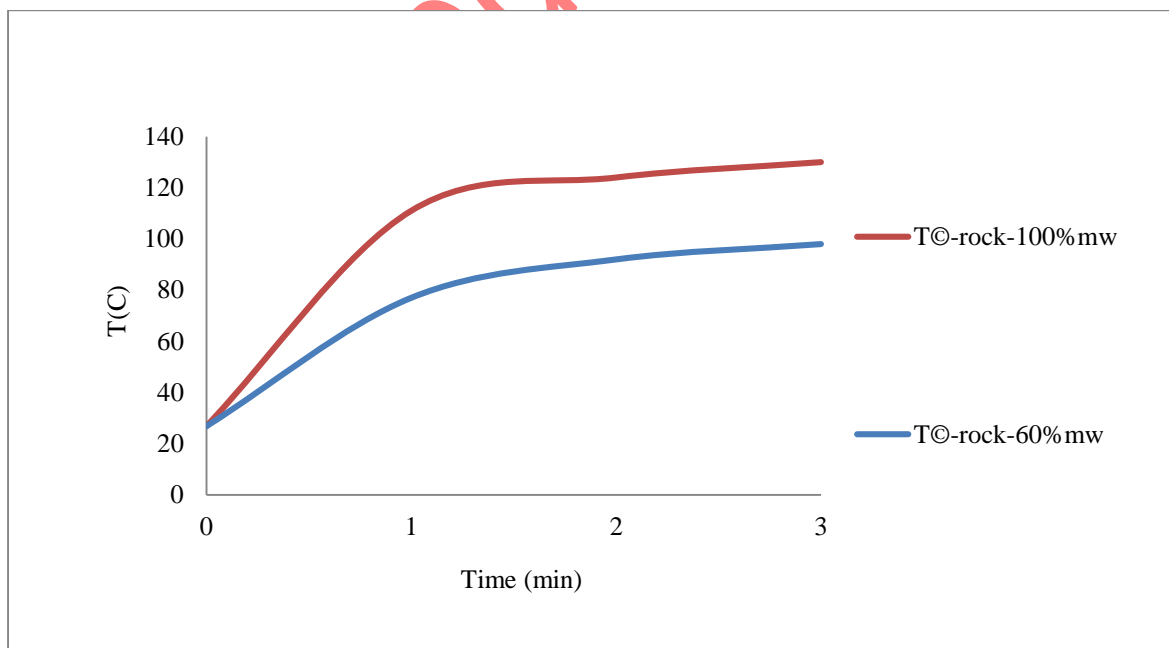
227 The temperature increase during microwave exposure is critical, as it can induce both physical and
228 chemical transformations in the adsorbed organic matter. Elevated temperatures may cause thermal
229 cracking of heavy polar hydrocarbon fractions, such as asphaltenes, leading to their desorption from
230 the rock surface. In addition, the breakdown of polar functional groups can modify the surface energy
231 of the rock, promoting a shift in wettability. These effects are particularly relevant in carbonate
232 reservoirs, where wettability alteration can significantly enhance oil recovery efficiency.

233 It should be noted that although the temperature rise observed under microwave exposure may appear
234 modest compared with conventional thermal methods (e.g., hot-water or steam flooding), the
235 underlying mechanism and spatial heating pattern are fundamentally different. Microwave heating is

286 characterized by volumetric and selective energy absorption, where electromagnetic energy is directly
287 absorbed by the material rather than being transferred via conduction or convection from an external
288 source. This leads to localized and highly efficient energy deposition in components with strong
289 microwave affinity [20].

290 Moreover, the apparently limited temperature increase recorded in this study should be interpreted
291 with caution. The surface temperature values were measured using a non-contact digital infrared
292 thermometer, which provides macroscopic surface readings rather than real-time volumetric internal
293 temperatures. Therefore, the internal temperature of the rock matrix may be considerably higher than
294 the measured surface temperature, particularly in zones with concentrated microwave absorption.

295 In summary, the enhanced temperature rise observed in the carbonate rock sections, as compared to
296 the crude oil, aligns with theoretical expectations based on the dielectric properties of the materials.
297 This localized heating effect plays a pivotal role in altering the physicochemical state of the adsorbed
298 hydrocarbons, thereby contributing to wettability modification and potentially improving hydrocarbon
299 displacement efficiency in carbonate formations.



300 Fig 2. Temperature changes of aged rock sections treated by microwave and [20]

301 3.2 Contact Angle

3.2.1 Contact Angle With Acidic Solution

According to the figure 3, the dataset presents a time-resolved measurement of contact angle evolution for three treated carbonate samples AFW, ASW, and ADW monitored over a 22-minutes period. Initially, all samples exhibit a contact angle of 132.535° , characteristic of a strongly oil-wet surface. As time progresses, the contact angles decrease at varying rates depending on the treatment type, indicating a wettability alteration process influenced by the nature of the aqueous phase.

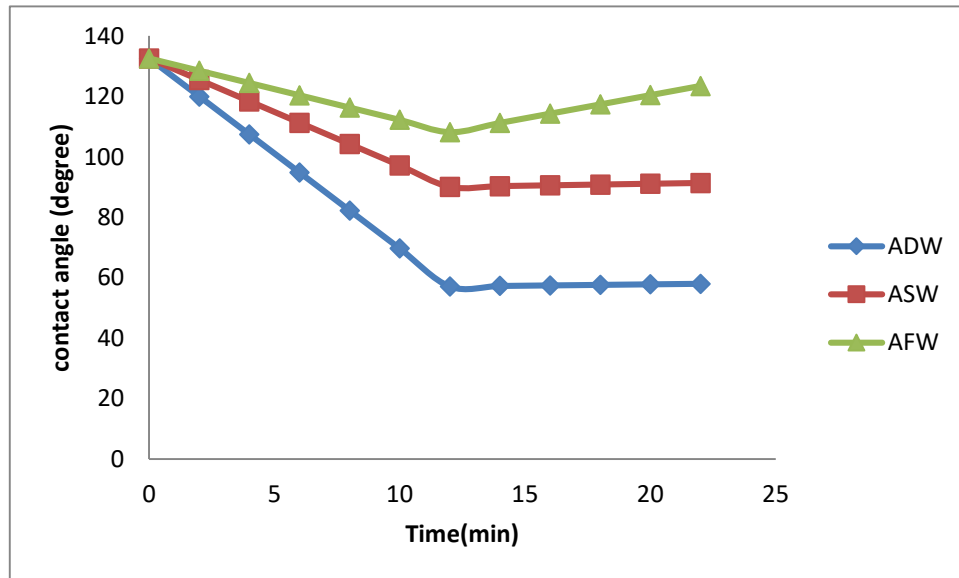
The ADW-treated sample exhibits the most pronounced reduction in contact angle, dropping sharply from 132.5° to 57.1° within the first few minutes of exposure. This substantial decrease reflects a rapid transition from oil-wet to water-wet conditions, likely resulting from the high reactivity of the acid in deionized water, which contains no competing ions to hinder surface reactions. Between 12 and 22 min, the ADW curve plateaus at approximately 58.0° , suggesting that the surface has reached a quasi-equilibrium state in terms of wettability alteration.

For the ASW-treated sample, a moderate reduction is observed: the contact angle decreases to 90.1° after 12 min, followed by a slight increase to 91.3° at 22 min. This behavior indicates partial wettability alteration, where seawater-derived divalent ions such as calcium and magnesium may buffer the acid reactivity and stabilize some adsorbed hydrocarbon species. The minor increase at later times likely reflects surface reorganization or re-adsorption of hydrophobic components.

The AFW-treated sample shows the least effective alteration, with the contact angle decreasing only to 108.2° after 12 min and then gradually increasing to 123.5° by 22 min. This trend suggests that the formation water either suppresses acid-rock interactions or promotes re-adsorption of hydrocarbons onto the mineral surface, leading to a reversal toward more oil-wet conditions. This behavior can be attributed to the specific ionic composition of formation water, which may contain reservoir-specific ions that reinforce the original surface characteristics.

Comparatively, the data clearly demonstrate that ADW treatment is the most effective in promoting water-wet conditions, followed by ASW, while AFW appears to hinder wettability alteration. The

327 observed trends underscore the critical influence of brine chemistry on acid-induced surface
328 modifications. These findings have significant implications for enhanced oil recovery operations,
329 where efficient wettability alteration can substantially improve oil displacement efficiency in
330 carbonate reservoirs.



331

332 Fig 3. The contact angle between aged rock sections and crude oil being treated with acidic solutions
333 Among the three, the ADW-treated sample exhibits the most significant and rapid reduction in contact
334 angle, dropping sharply to around 57° within the first hour. This indicates a highly efficient transition
335 from oil-wet to water-wet behavior. The pronounced decline can be attributed to the purity of
336 deionized water, which lacks interfering ions, thus enabling the hydrochloric acid to react unhindered
337 with the carbonate surface. This promotes the dissolution of surface-bound hydrocarbons and exposes
338 more hydrophilic mineral sites. After the first hour, the contact angle curve levels off, suggesting that
339 a chemical equilibrium has been reached and further acid-rock reaction is minimal.

340 In contrast, the ASW-treated sample shows a more moderate reduction in contact angle, stabilizing at
341 approximately 90°. This partial wettability alteration is likely due to the presence of divalent cations
342 such as Ca^{2+} and Mg^{2+} in synthetic seawater, which can compete with hydrogen ions during
343 acidization. These ions may form precipitates or passivate the rock surface, limiting further reaction

344 and hindering complete transition to water-wet conditions. The constant contact angle after the first
345 hour reflects a relatively stable interfacial state, where acid accessibility is chemically buffered.

346 The AFW-treated sample shows the least reduction in contact angle, with values remaining relatively
347 high and even increasing slightly after one hour. This trend is particularly noteworthy as it suggests a
348 reversal or suppression of wettability alteration. Formation water typically contains reservoir-specific
349 ions, high salinity, and sometimes organic compounds that can strongly adsorb onto the rock surface.
350 These constituents may block active sites, reduce acid effectiveness, or enhance the re-adsorption of
351 oil components, thereby maintaining or even reinforcing the oil-wet state. The mild increase observed
352 in the contact angle beyond the one-hour mark may be due to reorganization of surface-bound species
353 or a secondary adsorption process, possibly involving organic material from the formation water
354 itself.

355 In the ADW system, the acid is diluted in deionized water, which lacks dissolved ions. As a result, the
356 15wt% HCl remains highly reactive and unbuffered, enabling aggressive interaction with the
357 carbonate surface. This leads to rapid dissolution of the rock matrix, enhanced removal of surface-
358 bound hydrocarbons, and a strong shift toward water-wet conditions. Consequently, the contact angle
359 drops sharply from approximately 132° to 57° within the first hour, and then stabilizes indicating that
360 the rock-fluid interface has reached chemical and wetting equilibrium.

361 In contrast, the ASW solution contains a mixture of salts representative of synthetic seawater,
362 including divalent cations such as Mg^{2+} and Ca^{2+} , as well as monovalent ions like Na^+ and K^+ . These
363 ions influence the acid-rock interaction by buffering the reactivity of HCl and participating in surface
364 adsorption and complexation processes. The presence of magnesium and calcium ions in particular
365 can form precipitates or occupy active sites on the rock surface, reducing the extent of acid-driven
366 wettability alteration. As a result, the contact angle decreases more moderately, stabilizing at
367 approximately 90°, indicating a partial transition from oil-wet to mixed-wet or weakly water-wet
368 conditions.

369 The AFW treatment, involving formation water, introduces a highly complex ionic environment with
370 potentially high salinity and the presence of reservoir-specific ions and organic matter. These
371 constituents can inhibit the action of hydrochloric acid by saturating reactive sites or enhancing the re-
372 adsorption of oil components through ionic bridging or surface passivation. The contact angle in the
373 AFW system shows only a slight decrease, followed by a gradual increase after one hour, ultimately
374 stabilizing above 120°, suggesting that the surface remains dominantly oil-wet throughout the
375 experiment.

376 Overall, the trend observed in the graph highlights the critical role of brine composition in acid-
377 induced wettability alteration. The absence of interfering ions in ADW maximizes acid efficiency,
378 while the complex ionic environments in ASW and especially AFW reduce acid performance.
379 Understanding the interactions between acid, ions, and rock surfaces is essential for optimizing
380 stimulation fluids in carbonate reservoirs, where wettability alteration significantly influences oil
381 recovery efficiency.

382 In the ADW system, the acid is diluted with deionized water, containing no dissolved salts. This ion-
383 free medium allows the 15% HCl to remain in its most reactive and unbuffered form. As a result, HCl
384 reacts aggressively with the carbonate minerals, promoting rapid dissolution of calcite and effective
385 desorption of surface-bound oil films. This leads to a sharp decrease in contact angle from 132° to
386 approximately 57° within the first hour, reflecting a strong transition from oil-wet to water-wet
387 conditions. The absence of salts ensures that there is no competition at the mineral surface, allowing
388 complete exposure of hydrophilic sites.

389 In the ASW solution, the HCl is mixed with synthetic seawater containing, Sodium chloride (NaCl) A
390 monovalent salt that generally increases ionic strength but does not significantly compete with H⁺
391 ions. However, it can affect the electrical double layer at the rock-fluid interface. Magnesium chloride
392 (MgCl₂), A divalent salt with strong surface activity. Mg²⁺ can adsorb onto the carbonate surface or
393 form insoluble salts with carbonate ions, reducing acid access to reactive sites and buffering acid
394 reactivity. Sodium sulfate (Na₂SO₄), Sulfate ions (SO₄²⁻) can compete with carbonate or interact with

390 calcium to form gypsum or other precipitates, altering surface charge and potentially stabilizing oil
396 films. Calcium chloride (CaCl_2): A divalent salt that also reduces surface reactivity by occupying
397 active sites or forming precipitates with sulfate or carbonate ions. It plays a critical role in moderating
398 wettability alteration. Potassium chloride (KCl), A monovalent salt with lower surface activity than
399 divalent ions but contributes to overall ionic strength and potential clay swelling control if applicable.

400 These salts collectively buffer the HCl, reduce its reactivity with the rock, and compete for surface
401 adsorption, leading to only partial wettability alteration. Consequently, the contact angle for ASW-
402 treated samples stabilizes at around 90° , indicating an intermediate or mixed-wet state.

403 In the AFW system, which contains reservoir-derived formation water, the ionic composition is
404 typically complex and may include high concentrations of:

- 405 1- NaCl and CaCl_2 in large amounts, which buffer acid action and stabilize oil-wet conditions.
- 406 2- MgCl_2 , which can form precipitates or enhance surface charge shielding.
- 407 3- Organic matter and hydrocarbons, which may be present in trace quantities and promote the
408 re-adsorption of oil components onto the rock.

409 The interaction of these species with 15% HCl is more restrictive. The acid's reactivity is heavily
410 moderated, and the surface becomes resistant to full wettability alteration. The result is a relatively
411 high and stable contact angle above 120° , with a mild increase observed after 1 hour, likely due to re-
412 adsorption of hydrophobic species or secondary ionic interactions that reinforce oil-wet behavior.

413 In conclusion, the presence of specific salts in the acid solution has a profound effect on the efficiency
414 of wettability alteration. While ADW achieves the most significant wettability shift due to the absence
415 of interfering ions, the presence of NaCl, MgCl_2 , Na_2SO_4 , CaCl_2 , and KCl in ASW and AFW
416 diminishes acid effectiveness by buffering, surface site competition, precipitation reactions, and
417 possible organic interactions. Understanding the distinct chemical roles of each salt is essential for
418 tailoring acidizing fluids in carbonate reservoirs to maximize wettability modification and improve oil
419 recovery.

3.2.2 Contact Angle by Microwave

According to the figure 4 , the table presents a time-dependent comparison of contact angle measurements for surfaces exposed to microwave radiation at two different power levels, 780 watts and 1300 watts. Measurements were recorded over a 11-minute period at 1-minute intervals, capturing the evolution of surface wettability under varying energy inputs. All contact angles begin at high values (above 100°), indicating initially oil-wet surfaces, and progressively decrease over time, suggesting a shift toward more water-wet conditions as exposure continues.

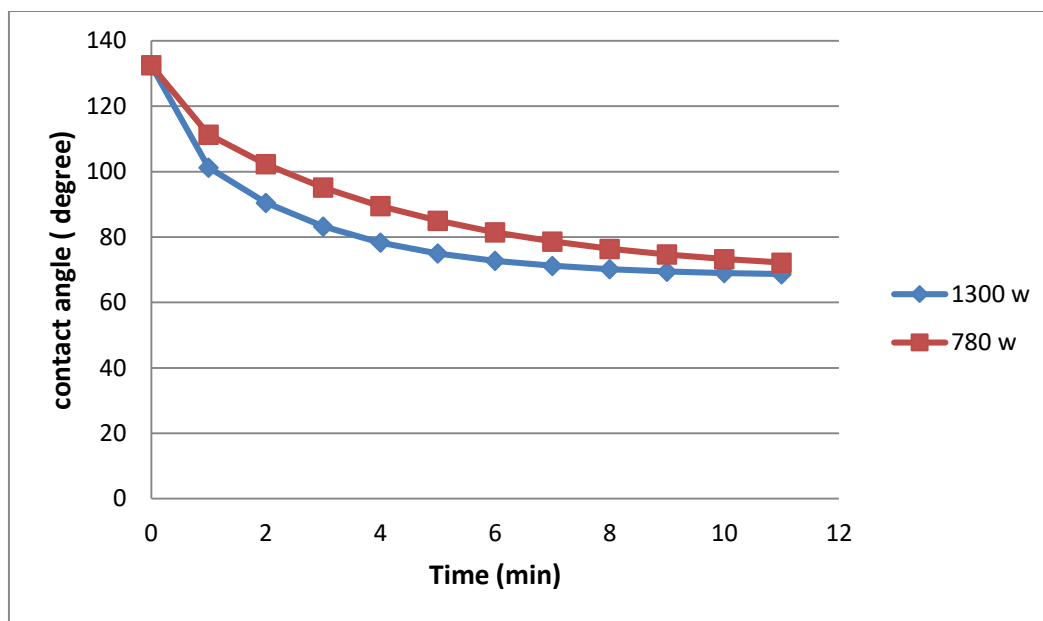
At 1 minutes, the contact angle is 111.354° for 780 W and 101.255° for 1300 W, reflecting the early stage of wettability alteration. By 30 minutes, the difference between the two treatments becomes more pronounced: the 1300 W condition results in a sharper decrease to 90.516° , compared to 102.309° for 780 W. This pattern continues consistently throughout the duration of the experiment.

As time progresses, the 1300 W treatment consistently produces lower contact angle values than the 780 W treatment at every time point. For example, at 6 minutes, the contact angle is 74.988° for 1300 W, whereas it remains at 85.003° for 780 W. By the end of the experiment at 11 minutes, the contact angle reaches 68.673° for 1300 W and 72.176° for 780 W.

This consistent difference illustrates a key phenomenon, higher microwave power results in a more rapid and more effective wettability alteration. The greater energy input likely enhances molecular agitation, accelerates surface reactions, and increases desorption of hydrophobic components, thereby facilitating a quicker transition from oil-wet to water-wet surface conditions.

Moreover, the rate of decrease is steeper during the first half of the experiment for both power levels, particularly between 1 and 11 minutes. This suggests that the majority of the microwave-induced surface reconfiguration occurs early in the exposure process. After about 6 minutes, the curves begin to flatten, indicating a gradual approach toward equilibrium where additional exposure contributes to only minor changes in contact angle.

εεε In conclusion, the data clearly show that microwave-assisted wettability alteration is power-
εεο dependent. The 1300 W treatment leads to faster and deeper reductions in contact angle, making it
εεϖ more effective for altering surface conditions in a shorter timeframe. This insight is especially
εεϗ valuable for applications such as enhanced oil recovery or surface treatment processes, where rapid
εελ and efficient wettability modification is desired.



εεε

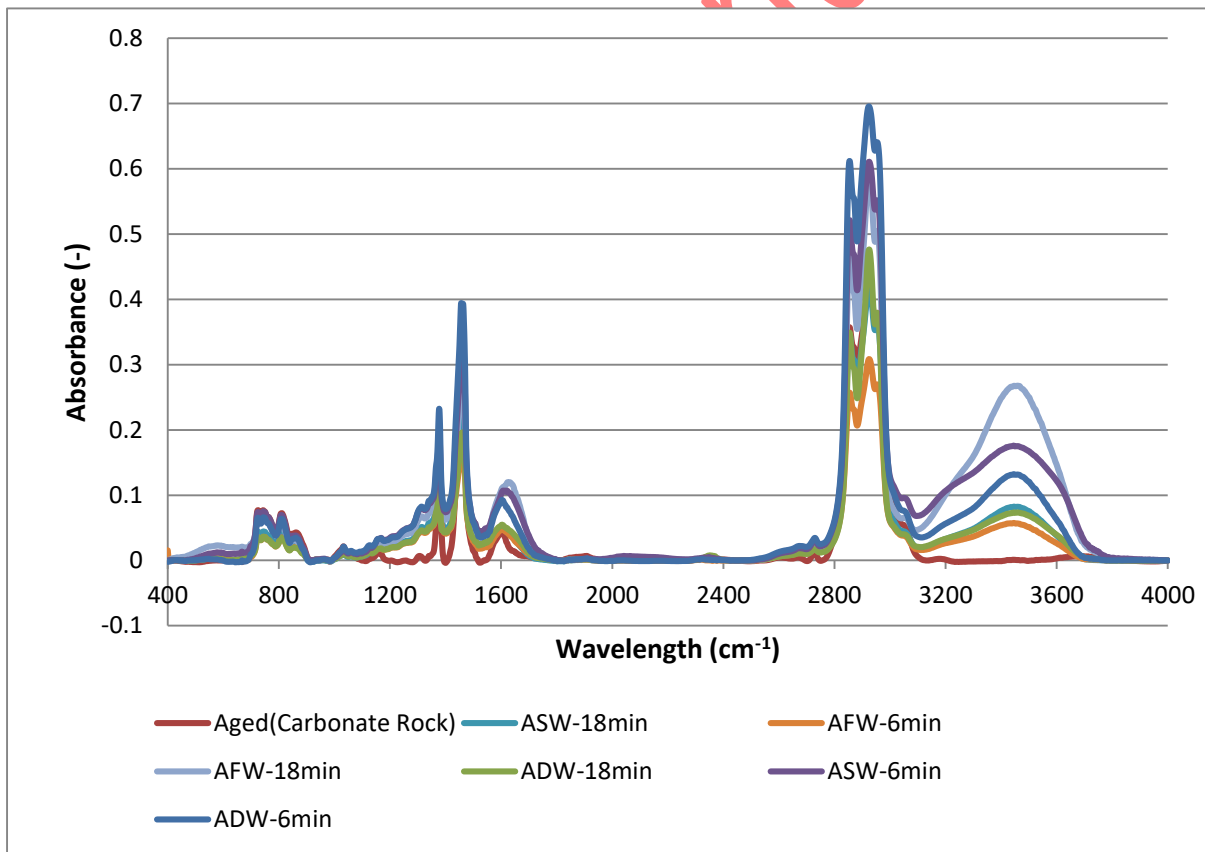
εεο Fig 4. The contact angle between rock sections and crude oil after being exposed to microwave.

εεο This study investigates the impact of microwave irradiation on wettability alteration of oil-wet rock
εεο surfaces under two different power settings , 780 W and 1300 W. The results demonstrate that higher
εεο microwave power significantly enhances the rate and extent of wettability transition, as evidenced by
εεο a faster and greater reduction in contact angle. At 1300 W, the contact angle drops more rapidly than
εεο at 780 W, indicating a more effective shift from oil-wet to water-wet conditions. This improved
εεο performance is attributed to intensified dielectric heating, which promotes molecular agitation,
εεο thermal desorption of surface-bound hydrocarbons, and surface energy reorganization. Most of the
εεο contact angle reduction occurs within the first 6 minutes of exposure, suggesting that key surface
εεο transformations take place early in the treatment. Beyond this point, the system tends toward
εεο equilibrium, with only marginal changes observed. Overall, these findings underscore the importance
εεο of microwave power intensity in controlling wettability dynamics and support the application of

462 microwave-assisted methods in enhanced oil recovery and surface conditioning, where efficient fluid-
463 rock interaction is critical to improving hydrocarbon recovery.

464 3.3 ATR-FTIR spectroscopy

465 The contact angles, measured using the sessile drop technique, were employed to assess the
466 wettability of the treated rock sections. However, no information was provided regarding the
467 desorption of hydrocarbons from the rock surface. To investigate the chemical changes on the surface
468 of the rock and the behavior of adsorbed hydrocarbons, the ATR-FTIR spectra of the acid-treated rock
469 sections are presented in Fig. 5. Additionally, Fig. 6 shows the ATR-FTIR spectra of rock sections
470 treated with both acid solution and microwave radiation at 780 W and 1300 W, respectively.



472 Fig 5. The normalized ATR-FTIR spectrums for acidized rock sections

473

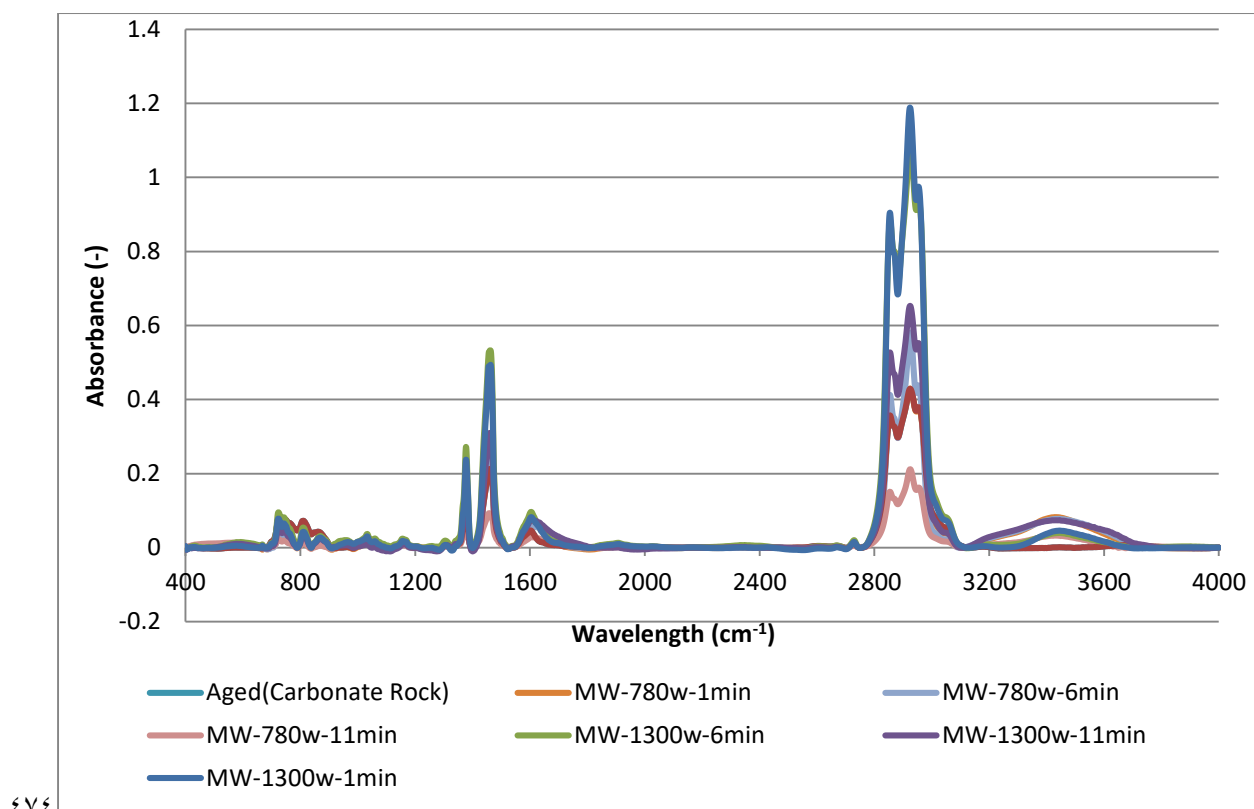


Fig 6. The normalized ATR- FTIR spectrums for crude section and sections treated by the microwave radiation power

The peaks observed in the ATR-FTIR spectra represent both the hydrocarbons adsorbed on the rock surface and the minerals within the rock. These peaks can be categorized into three groups: rock-related, hydrocarbon-related, and common peaks. Since the primary focus of the ATR-FTIR spectra was on the hydrocarbon chemistry, only those peaks specifically associated with hydrocarbons were considered in the analysis. As shown in Table 5, the aliphatic C-H bonds are characterized by peaks within the range of 2755-3000 cm^{-1} . Additionally, the ranges of 3000-3100 cm^{-1} and 1566-1668 cm^{-1} correspond to the C-H and C=C bonds in aromatic rings, respectively. Ketone-based functional groups, including carboxylic acid groups, exhibit vibrations in the 1668-1800 cm^{-1} range. The amine and alcohol functional groups appear in the 3100-3500 cm^{-1} range. More detailed information on hydrocarbon chemistry can be found in Table 5. As previously mentioned, the characteristic indexes provided by Tanhaei et al. (2023) were used to extract numerical data from the ATR-FTIR spectra. [20,27,28]. The Aromatic/Aliphatic, Aliphatic Length, C=O/Aliphatic, C=O/Aromatic,

489 Polar/Aliphatic, and Polar/Aromatic indices were determined based on the integral areas of the
490 corresponding peaks. The characteristic indices (Acidic Solution) derived from the ATR-FTIR spectra
491 are presented in Table 6.

492 Table 5. The assignments of the peaks in the ATR-FTIR spectrums [24,25,28].

Wavelength	Assignment
3100-3500	N-H, O-H
3000-3100	C-H stretch in aromatic
2946-3000	CH ₃ asymmetric stretch
2881-2946	CH ₂ asymmetric stretch
2755-2881	CH ₂ symmetric Stretch
1668-1800	C=O stretch in ketones, aldehydes, and carboxylic acids
1566-1668	Aromatic C=C stretch

493 To investigate the chemistry of the hydrocarbons, which have a greater tendency for desorption from
494 the rock surface, the ATR-FTIR spectrums were analyzed from an analytical point of view. In this
495 regard, the integral area of each hydrocarbon-assigned peak was employed to be used in the
496 characteristic equations given by Tanhaei et al .2023 [20,28]. Equations 1-6 show the ratios used to

497 characterize the chemistry of hydrocarbons adsorbed on the rock surface. In Equations 1-6, the 'A_i'
 498 stands with the integral area below the peak in the range of 'i'.

$$C=O/A_{\text{Aliphatic}} = \frac{A_{1668-1800}}{A_{2881-2946}} \quad (1)$$

$$C=O/A_{\text{Aromatic}} = \frac{A_{1668-1800}}{A_{1566-1668}} \quad (2)$$

$$A_{\text{Aromatic}}/A_{\text{Aliphatic}} = \frac{A_{1566-1668}}{A_{2881-2946}} \quad (3)$$

$$A_{\text{Aliphatic length}} = \frac{A_{2946-3000}}{A_{2881-2946}} \quad (4)$$

$$Polar/A_{\text{Aliphatic}} = \frac{A_{3100-3500}}{A_{2881-2946}} \quad (5)$$

$$Polar/A_{\text{Aliphatic}} = \frac{A_{3100-3500}}{A_{2881-2946}} \quad (6)$$

499

500 Table 6. The characteristic indexes calculated from the ATR-FTIR spectrums of the crude and acid-
 501 treated rock section (HCl 15%)

Acidic solution	Time(min)	Aliphatic			Polar/Aliphatic	Polar/Aromatic
		C=O/Aliphatic	C=O/Aromatic	Aromatic/Aliphatic		
ADW	6	0.197755	0.326208	0.611396	3.038896	5.290352
ADW	18	0.215396	0.312785	0.690783	2.521153	3.806541
ASW	6	0.136844	0.304551	0.437237	4.095579	10.02738
ASW	18	0.102712	0.27272	0.368589	4.476024	12.57007
AFW	6	0.204071	0.33433	0.613652	3.019946	5.25516
AFW	18	0.227082	0.32781	0.694957	2.486096	3.741435

0.2 The presented table 6, offers a detailed quantitative analysis of ATR-FTIR-derived chemical indices
0.3 that reflect molecular-level changes on carbonate rock surfaces treated with 15% hydrochloric acid
0.4 (HCl) in different aqueous solutions ADW (acid in deionized water), ASW (acid in synthetic
0.5 seawater), and AFW (acid in formation water)—at three time intervals, 20 and 60 minutes. These
0.6 solutions contain varying combinations of key inorganic salts such as sodium chloride (NaCl),
0.7 potassium chloride (KCl), calcium chloride (CaCl₂), magnesium chloride (MgCl₂), and sodium
0.8 sulfate (Na₂SO₄), which significantly influence acid–rock interaction and surface chemistry during
0.9 treatment.

1.0 For the ADW system, which contains no dissolved salts, the acid remains highly active and
1.1 unbuffered. This enables free interaction with carbonate minerals, promoting strong decarbonation
1.2 and dissolution processes. Over time, the increase in C=O/Aliphatic and C=O/Aromatic ratios (from
1.3 0.197 to 0.221 and 0.326 to 0.307 respectively) indicates the gradual breakdown of polar oxygen-
1.4 containing groups and aliphatic chains, with partial oxidation of surface-bound hydrocarbons. The
1.5 Aromatic/Aliphatic ratio increases notably from 0.61 to 0.72, suggesting selective degradation of
1.6 aliphatic components, leaving more stable aromatic structures. Simultaneously, Polar/Aliphatic and
1.7 Polar/Aromatic ratios decrease steadily, reflecting the overall reduction in polarity as the surface
1.8 becomes cleaner and less hydrocarbon-saturated.

1.9 In the ASW system, where HCl is mixed with synthetic seawater containing NaCl, MgCl₂, CaCl₂,
2.0 Na₂SO₄, and KCl, distinct chemical behavior is observed. These salts, particularly the divalent cations
2.1 (Ca²⁺, Mg²⁺), can buffer HCl activity, precipitate on mineral surfaces, and compete for adsorption
2.2 sites. The C=O/Aliphatic ratio shows a strong decrease from 0.137 to 0.090 over time, reflecting
2.3 limited acid accessibility and partial surface deactivation. The Aromatic/Aliphatic ratio drops from
2.4 0.437 to 0.344, indicating slower degradation of surface hydrocarbons, possibly due to salt shielding
2.5 or inhibition of polar group removal. Interestingly, the Polar/Aromatic and Polar/Aliphatic indices
2.6 increase with time, reaching 13.48 and 4.61 at 11 minutes. This suggests a higher retention or

027 exposure of polar functionalities, potentially due to sulfate complexation and limited desorption in the
028 presence of seawater ions.

029 For the AFW system, composed of formation water and 15% HCl, the complex ionic composition
030 (high salinity with NaCl, CaCl₂, MgCl₂, and possibly organic residues) alters the interaction further.

031 The C=O/Aliphatic and C=O/Aromatic ratios increase slightly over time, indicating slower oxidation
032 and a less aggressive acid attack, likely due to ion competition or saturation of reactive sites. The
033 Aromatic/Aliphatic ratio increases from 0.61 to 0.72, which is consistent with partial removal of
034 aliphatic chains. However, compared to ADW, the reduction in Polar/Aliphatic and Polar/Aromatic
035 indices is less pronounced, and their final values (2.29 and 3.20) remain higher, suggesting that
036 surface cleaning is less complete. This may be attributed to persistent ion interference or re-adsorption
037 of organics facilitated by divalent ions and high ionic strength.

038 In summary, the data clearly show that ionic composition of the solution plays a crucial role in acid–
039 rock chemical interactions. The ADW system, free of salts, exhibits the most effective hydrocarbon
040 removal and wettability alteration. In contrast, the ASW and AFW systems, containing salts such as
041 NaCl, KCl, CaCl₂, MgCl₂, and Na₂SO₄, demonstrate suppressed acid reactivity, limited surface
042 cleaning, and altered surface functionality due to competitive adsorption, buffering effects, and
043 possible precipitation. These findings are critical for optimizing acidizing fluid design in carbonate
044 reservoirs, where controlling surface chemistry directly impacts wettability, permeability, and overall
045 recovery efficiency.

046 The dataset presents of table 7, the detailed chemical analysis of surface changes induced by
047 microwave irradiation on carbonate rock samples treated at two different power levels 780 watts and
048 1300 watts over exposure durations of 1, 6, and 11 minutes. The table includes a set of molecular
049 indices derived from ATR-FTIR spectroscopy, which provide insight into the evolution of surface
050 functionality, polarity, and hydrocarbon composition. These results have significant implications in
051 the context of petroleum engineering and chemical surface modification, particularly for enhanced oil
052 recovery (EOR) processes.

003 For the 780 W treatment, the contact surface shows a gradual and consistent increase in aromatic
004 character and polarity with exposure time. The C=O/Aliphatic ratio decreases from 0.1711 to 0.1555,
005 suggesting partial breakdown of oxygenated aliphatic compounds or desorption of less stable polar
006 species. Simultaneously, the C=O/Aromatic ratio slightly increases, implying that aromatic structures
007 retain or accumulate polar functionalities more effectively under lower-energy microwave exposure.
008 The Aromatic/Aliphatic ratio rises from 0.5447 to 0.6161, indicating preferential degradation of
009 aliphatic hydrocarbons and relative enrichment of aromatic groups. Additionally, the Polar/Aliphatic
010 and Polar/Aromatic ratios also increase with time, reflecting an overall enhancement in surface
011 polarity. These trends suggest that 780 W microwave energy facilitates gradual desorption and
012 molecular rearrangement on the rock surface, but does not completely eliminate polar and
013 hydrocarbon content.

014 In contrast, the 1300 W treatment results in more aggressive and efficient molecular transformations.
015 The C=O/Aliphatic ratio drops significantly from 0.1623 to 0.1228, indicating a more extensive
016 removal of oxygen-containing aliphatic species. Likewise, the Aromatic/Aliphatic ratio decreases
017 from 0.4885 to 0.4096, suggesting deeper structural degradation of hydrocarbons, affecting both
018 aliphatic and aromatic components. Importantly, the Polar/Aliphatic and Polar/Aromatic indices
019 decline markedly from 3.1981 and 6.4107 to 1.9946 and 4.7383, respectively. This reflects a
020 significant reduction in surface polarity, likely due to efficient desorption of polar organic matter and
021 transformation of the surface to a more mineral-dominated, less hydrocarbon-saturated state.

022 From a microwave physics perspective, higher power (1300 W) delivers greater electromagnetic
023 energy, which translates into stronger dielectric heating. This enhances molecular vibration, promotes
024 bond cleavage, and facilitates thermal desorption and decomposition of organic films adhered to the
025 rock surface. The selective and volumetric heating characteristics of microwaves at this power level
026 enable more uniform and deeper interaction with the porous structure of carbonates, leading to more
027 complete surface cleaning and wettability alteration.

078 In the context of petroleum engineering, these findings are highly significant. The observed reduction
 079 in polar indices and aliphatic content indicates that higher microwave power increases the exposure of
 080 hydrophilic mineral surfaces, thereby promoting water-wet conditions a desirable outcome for
 081 enhancing oil displacement efficiency in carbonate reservoirs. Moreover, the results suggest that
 082 microwave-assisted treatments can be effectively optimized by adjusting the irradiation power and
 083 exposure time to achieve the desired surface chemistry under specific reservoir conditions.

084 Table 7. The characteristic indexes calculated from the ATR-FTIR spectrums of the treated rock
 085 section, which by microwave

Time(min)	Power(w)	C=O/Aliphatic c	C=O/Aromatic c	Aromatic/Aliphatic c	Aliphatic length	Polar/Aliphatic c	Polar/Aromatic c
1	780W	0.171148	0.344926	0.54471	0.395107	4.004907	7.325382
6	780W	0.162057	0.349471	0.5862	0.426341	4.559309	7.774894
11	780W	0.155496	0.352752	0.616148	0.448887	4.959493	8.099366
1	1300W	0.162257	0.346277	0.488514	0.374775	3.198058	6.410718
6	1300W	0.139356	0.35292	0.442712	0.374425	2.499141	5.439437
11	1300W	0.122825	0.357715	0.409651	0.374173	1.994642	4.738336

086 In conclusion, the analysis clearly shows that microwave power intensity plays a pivotal role in
 087 governing the chemical and physical evolution of carbonate rock surfaces. While 780 W results in
 088 moderate, progressive surface modification, 1300 W achieves a more substantial and efficient
 089 transformation, making it more effective for applications aimed at wettability alteration, hydrocarbon
 090 desorption, and formation stimulation. These findings support the integration of high-power
 091 microwave technologies in advanced EOR strategies and surface treatment systems.

092 4. Conclusion

093 In this research, comprehensively investigated the independent effects of microwave irradiation and
 094 acidic fluids on wettability alteration and hydrocarbon desorption in carbonate reservoir rocks.
 095 Through a series of contact angle measurements and ATR-FTIR spectroscopic analyses, it was

096 demonstrated that both treatments significantly impact the rock-fluid interface, albeit through
097 different mechanisms.

098 • Microwave irradiation particularly at 1300 W for up to 11 minutes proved highly effective in
099 reducing the contact angle from 132.5° to 68.7°, indicating a substantial transition toward
100 water-wet conditions. This effect is attributed to dielectric heating, which facilitates the
101 thermal desorption of polar and aromatic hydrocarbon compounds, as evidenced by the
102 observed decreases in the Polar/Aliphatic and Aromatic/Aliphatic indices in the FTIR
103 spectra.

104 • Acid treatment with 15 wt% HCl, particularly when prepared in deionized water (ADW),
105 exhibited the greatest wettability alteration, reducing the contact angle to 57.1°. In contrast,
106 the presence of ions in synthetic seawater (ASW) and formation water (AFW) decreased the
107 acid's effectiveness due to buffering effects, surface passivation, and precipitation reactions.
108 These trends were further supported by ATR-FTIR spectroscopy, which revealed more
109 extensive desorption of hydrocarbon compounds in the ADW-treated samples. Specifically,
110 the ADW system showed a pronounced decrease in the Polar/Aliphatic and Polar/Aromatic
111 indices over time, indicating efficient removal of polar functional groups and surface-bound
112 hydrocarbons. Conversely, the ASW and AFW treatments displayed higher polarity indices
113 and smaller variations in aliphatic and aromatic signatures, suggesting incomplete surface
114 cleaning and persistent hydrocarbon retention.

115 Importantly, the results revealed that while both microwave energy and acid solutions independently
116 enhance wettability alteration, their combination yields superior performance particularly in complex
117 reservoir environments where salinity and organic deposition limit conventional acidizing efficiency.
118 These findings offer valuable insights for designing advanced enhanced oil recovery (EOR)
119 techniques and support the integration of microwave-assisted stimulation as a complementary strategy
120 to traditional acidizing methods in carbonate reservoirs.

121

References

- [1] Garrouch, Ali A., and Alfred R. Jennings Jr. "A contemporary approach to carbonate matrix acidizing." *Journal of Petroleum Science and Engineering* 158 (2017): 129-143, <https://doi.org/10.1016/j.petrol.2017.08.045> .
- [2] Rabbani ,R., Davarpanah,A. , Memariani,M . “ An experimental study of acidizing operation performances on the wellbore productivity index enhancement”, *J.of.Teh.*, (2019), DOI: [10.1007/s13202-018-0441-8](https://doi.org/10.1007/s13202-018-0441-8).
- [3] Wu, Yahong, et al. "Application of VES acid system on carbonate rocks with uninvasion matrix for acid etching and fracture propagation." *Processes* 7.3 (2019): 159, <https://doi.org/10.3390/pr7030159>.
- [4] Yoo, Hyunsang, et al. "An experimental study on acid-rock reaction kinetics using dolomite in carbonate acidizing." *Journal of Petroleum Science and Engineering* 168 (2018): 478-494, DOI: [10.1016/j.petrol.2018.05.041](https://doi.org/10.1016/j.petrol.2018.05.041).
- [5] Fan, Yu, et al. "Experimental study of the influences of different factors on the acid-rock reaction rate of carbonate rocks." *Journal of Energy Storage* 63 (2023): 107064 , <https://doi.org/10.1016/j.est.2023.107064>.
- [6] Saeedi Dehaghani, Amir Hossein, and Mohammad Amin Behnam Motlagh. "Experimental Investigation of Foam Stability under Various Salinity Levels, Oil Types, and Surfactant Conditions: Effect of Natural Polymer Lignin." *Scientia Iranica* (2025) , [10.24200/sci.2025.66165.9885](https://doi.org/10.24200/sci.2025.66165.9885).
- [7] Parandeh, M., H.Z. Dehkohneh, and B.S. Soulgani, Experimental investigation of the acidizing effects on the mechanical properties of carbonated rocks. *Geoenergy Science and Engineering*, (2023) , <https://doi.org/10.1016/j.geoen.2023.211447> .

- 740 [8] Yoo, Hyunsang, and Jeonghwan Lee. "An experimental study on the optimum injection rate
746 for matrix acidizing in carbonate reservoirs." *Journal of the Korean Society of Mineral and*
747 *Energy Resources Engineers* 56.3 (2019): 227-238, DOI: [10.32390/ksmer.2019.56.3.227](https://doi.org/10.32390/ksmer.2019.56.3.227).
- 748 [9] He, Leping, et al. "Structural failure process of schistosity rock under microwave radiation at
749 high temperatures." *Fracture and Structural Integrity* 13.50 (2019): 649-657, DOI: [10.3221/IGF-
750 ESIS.50.55](https://doi.org/10.3221/IGF-ESIS.50.55).
- 751 [10] Mozafari, M., Nasri, A. "Experimental study of Iranian heavy crude oil heating under
752 microwave radiation", *J. of Teh.*, 35(1) (2016), DOI: [10.1016/j.petro.2017.01.028](https://doi.org/10.1016/j.petro.2017.01.028).
- 753 [11] Eskandari, S., Jalalhosseini, S.M. "Microwave Heating as an Enhanced Oil Recovery
754 Method—Potentials and Effective Parameters", *J. Petr. Eng.*, Tehran, Iran (2018), DOI:
755 [10.1080/15567036.2011.592906](https://doi.org/10.1080/15567036.2011.592906).
- 756 [12] Hong, L., Yucheng, G., Qijun, H., et al. Structural failure process of schistosity rock under
757 microwave radiation at high temperatures (2019), DOI: [10.3221/IGF-ESIS.50.55](https://doi.org/10.3221/IGF-ESIS.50.55).
- 758 [13] Taheri-Shakib, J., Shekarifarda, A., Naderi, N. "The study of Influence of electromagnetic
759 waves on the wettability alteration of oil-wet calcite: Imprints in surface properties", *J. Anal.*
760 *Appl. Pyrolysis.*, 127, pp. 176: 186 (2018), DOI: [10.3997/2214-4609.201901444](https://doi.org/10.3997/2214-4609.201901444).
- 761 [14] Karami, S., Dehaghani, A.H.S., Haghghi, M. "Investigation of smart water imbibition
762 assisted with microwave radiation as a novel hybrid method of enhanced oil recovery", *J. Mol.*
763 *Liq.*, 335, 116101(2021), DOI: [10.1016/j.molliq.2021.116101](https://doi.org/10.1016/j.molliq.2021.116101).
- 764 [15] Shang, H., Yue, Y., Zhang, J., et al. "Effect of microwave irradiation on the viscosity of
765 crude oil: A view at the molecular level", *J. Fuel. Proc. Tec.*, 170, 44-52(2018), DOI:
766 [10.1016/j.fuproc.2017.10.021](https://doi.org/10.1016/j.fuproc.2017.10.021).

- ٦٦٧ [16] Karami, S., Dehaghani,A.H.S. and Mousavi,A.H. “Condensate blockage removal using
٦٦٨ microwave and ultrasonic waves: Discussion on rock mechanical and electrical properties”, J. Pet.
٦٦٩ Sci. and Eng.,193, 107309(2020) , DOI: [10.1016/j.petrol.2020.107309](https://doi.org/10.1016/j.petrol.2020.107309).
- ٦٧٠ [17] Karami,S., Dehaghani,A.H.S, and Haghghi,M. “Analytical investigation of asphaltene
٦٧١ cracking due to microwave and ultrasonic radiations: A molecular insight into asphaltene
٦٧٢ characterization and rheology”, J.Geo. Sci. and Eng., 212481(2023) , DOI:
٦٧٣ [10.1016/j.geoen.2023.212481](https://doi.org/10.1016/j.geoen.2023.212481).
- ٦٧٤ [18] Mutyala, S., Fairbridge, C., Paré ,J.J. , et al.“ Microwave applications to oil sands and
٦٧٥ petroleum: A review”, Fuel .Proc. Tec.,91(2,127-35(2010), DOI: [10.1016/j.fuproc.2009.09.009](https://doi.org/10.1016/j.fuproc.2009.09.009).
- ٦٧٦ [19] Wang ,W., Han, P., Lu, X. “Effects of ultrasound on oily sludge deoiling”, J. haz. Mat.,
٦٧٧ 171(1-3),914-7(2009) , DOI: [10.1016/j.jhazmat.2009.06.091](https://doi.org/10.1016/j.jhazmat.2009.06.091).
- ٦٧٨ [20] Tanhaei, H., Saeedi Dehaghani, A. H., & Karami, S. Investigation of microwave radiation in
٦٧٩ conjugate with acidizing as a novel hybrid method of oil well stimulation. J. *Scientia Iranica*(
٦٨٠ 2023), [10.24200/sci.2023.62586.7985](https://doi.org/10.24200/sci.2023.62586.7985).
- ٦٨١ [21] Le, T. M., Nguyen, G. T., Dat, N. D., & Tran, N. T. (2023). An innovative approach based
٦٨٢ on microwave radiation for synthesis of zeolite 4A and porosity enhancement. *Results in*
٦٨٣ *Engineering*, 19, 101235 , DOI: [10.1016/j.rineng.2023.101235](https://doi.org/10.1016/j.rineng.2023.101235).
- ٦٨٤ [22] Hadi Tanhaei, Amir Hossein Saeedi Dehaghani, Independent effects of microwave
٦٨٥ irradiation and acidic solutions on asphaltene content and upgrading of heavy crude oil, Journal
٦٨٦ of Molecular Liquids, (2025) , <https://doi.org/10.1016/j.molliq.2025.127743>.
- ٦٨٧ [23] Tanhaei, H., Saeedi Dehaghani, A.H. Improvement of the quality of heavy crude oil and
٦٨٨ reducing the concentration of asphaltene hydrocarbons using microwave radiation during
٦٨٩ acidizing. *Sci Rep* **15**, 7434 (2025) , <https://doi.org/10.1038/s41598-025-91932-x>.

- 790 [24] Karami, S., Dehaghani, AHS., "A molecular insight into cracking of the asphaltene
791 hydrocarbons by using microwave radiation in the presence of the nanoparticles acting as
792 catalyst", J. Mol. . 364 ,120026(2022) , DOI: [10.1016/j.molliq.2022.120026](https://doi.org/10.1016/j.molliq.2022.120026).
- 793 [25] Zhang ,Y., Adam, M., Hart, A. , et al. "Impact of oil composition on microwave heating
794 behavior of heavy oils", J.Ene & Fue, 32(2),1592-9(2018) ,
795 <https://pubs.acs.org/doi/10.1021/acs.energyfuels.7b03675>.
- 796 [26] Scotti, R., Montanari, L." Molecular structure and intermolecular interaction of asphaltenes
797 by Structures and dynamics of asphaltenes", Springer. p. 79-113(1998) , DOI:[10.1007/978-1-](https://doi.org/10.1007/978-1-4899-1615-0_3)
798 [4899-1615-0_3](https://doi.org/10.1007/978-1-4899-1615-0_3).
- 799 [27] Hemmati-Sarapardeh, A., Dabir, B., Ahmadi ,M., et al. "Toward mechanistic understanding
800 of asphaltene aggregation behavior in toluene: The roles of asphaltene structure, aging time,
801 temperature, and ultrasonic radiation",J. Mol.Liq., 264,410-24(2018) , DOI:
802 [10.1016/j.molliq.2018.04.061](https://doi.org/10.1016/j.molliq.2018.04.061).
- 803 [28] Zhu, X., Su, M., Tang, S., et al. "Synthesis of thiolated chitosan and preparation
804 nanoparticles with sodium alginate for ocular drug delivery", Mol.vis.,18,1973(2012),
805 <https://doi.org/10.1021/acs.energyfuels.7b03675>.
- 806 [29] Scotti, R., and L. Montanari. "Molecular structure and intermolecular interaction of
807 asphaltenes by FT-IR, NMR, EPR." *Structures and dynamics of asphaltenes*. Boston, MA:
808 Springer US, 1998. 79-113. https://doi.org/10.1007/978-1-4899-1615-0_3.
- 809 [30] Tanhaei, H., Dehaghani, A. H. S., & Motlagh, M. A. B. (2024). A Review of waste
810 management approaches to maximise sustainable value of waste from the oil and gas industry. In
811 *The 2nd National and 1st International Conference on Environmental Challenges (Tarbiat*
812 *Modares University, 2024)*, <https://civilica.com/doc/2034996>.

813